Spiking voltages for faster switching of nematic liquid-crystal light modulators

Xiaodong Xun, Doo Jin Cho, and Robert W. Cohn

Electrical address circuits developed for driving fast-switching ferroelectric liquid-crystal spatial light modulators (SLM) can be programmed to increase the speed of much slower responding nematic liquid-crystal SLMs. Using an addressing circuit that can switch as fast as 0.164 ms, voltages are programmed for values of phase that exceed the desired phase, and when the phase reaches the desired value, the voltage is switched to the required steady-state voltage. For a SLM that has a phase range of 3.5π and that is programmed over a 2π range, switching speed is reduced from 400 ms to between 71 and 77 ms. The speedup algorithm is applied to each pixel of the SLM together with a digital correction for a spatially nonuniform phase.

OCIS codes: 230.6120, 230.3720, 050.1970, 070.2580.

1. Introduction

Parallel aligned nematic liquid-crystal (NLC) spatial light modulators. (SLMs) are useful as continuous analog phase modulators for programmable diffractive optics. However, the NLC typically switches at much slower speeds than the binary-switching ferroelectric liquid crystal (FLC). The specified switching speed for the Boulder Nonlinear Systems (BNS) 512×512 pixel SLM filled with FLC is <450 μs and filled with 2π thick NLC for visible wavelengths the switching speed is less than 100 ms.[1] The electrical address circuit for this SLM has a frame loading speed of 164 μs, which greatly exceeds the switching speed of NLC, thereby providing an added degree of control, which we propose to use to increase the switching speed.

Previously reported methods for increasing the switching speed include pi-cells,[2] dual frequency addressing,[3] and the transient nematic effect.[4] These methods, which require specially oriented LC or special voltage signals, are capable of switching NLC at submillisecond rates, but are not available to the end users of the specific SLM reported herein. The switching speed of this custom SLM is not only slower than that achieved for specialty LC cells,[2–4] but (due to an extra thick layer of NLC and extra capacitance due to the inclusion of an experimental backplane mirror[5]) the switching speed is even slower than the published specifications[1] or than in published reports[6,7] for the standard BNS SLM. Our proposed speedup method does not approach the switching speeds of the specialty cells,[2–4] but it does approach the speed of the standard SLM. Therefore the purpose of this paper is to show how high rate address circuits can be programmed to increase the switching speed of NLC SLMs.

The approach used to speed up the SLM is simply to drive the NLC with an address voltage that exceeds the steady-state voltage required to maintain the desired value of phase. Then when the desired phase value is reached, the voltage is set to the steady-state voltage. For example, in Fig. 1 a spiking voltage V_{s2} if held indefinitely would produce the steady-state phase φ_{s2}. However, the voltage is switched at time t_s to V_B to realize the desired phase φ_B faster than if the voltage V_B (instead of V_{s2}) had initially been applied (as illustrated in the lowest curve in Fig. 1). We refer to this overdriving of the NLC as "spiking." In our method the transient behavior of the SLM is measured and these data are used with an algorithm that selects the appropriate spiking pulse for each pixel of the SLM. We believe this is the first report of a transient speedup "calibration" for the programming of arbitrary patterns on a phase-only SLM. Furthermore, the speedup calibra-

When this research was performed, the authors were with the ElectroOptics Research Institute and Nanotechnology Center, University of Louisville, Louisville, Kentucky 40292. D. J. Cho is now with the Department of Physics, Ajou University, SuWon, 443-749, South Korea. R. W. Cohn's e-mail address is rwcohn@uofl.edu.

Received 4 May 2005; revised 19 August 2005; accepted 7 September 2005.

0003-6935/06/133136-08$15.00/0

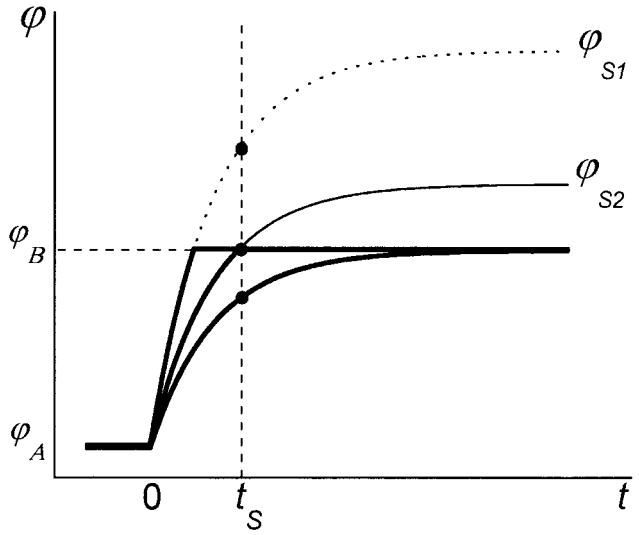

Fig. 1. Schematic for explaining the choice of spiking voltage versus switching time t_s.

tion is compatible (and used in the results reported herein) with a calibration method that corrects for a nonflat spatial phase across the SLM.[8]

2. Background and Assumptions

In Section 3 we present measurements of the steady-state and transient phase response of the SLM. From the fitting of numerical models to these measurements (Section 4) it is possible to design a speedup algorithm (Section 4), which is demonstrated in Section 5. That is to say, the speedup algorithm is strictly based on empirical measurements and treating the SLM as a so-called "black box."

Before presenting the measurements it may prove helpful to first consider a few points about the characteristics of NLC and the SLM. These are useful both to understand the characteristics of the measurements and the limitations placed on the user in developing speedup algorithms.

(1) Each pixel of the SLM is digitally addressed from a personal computer with grayscale values G between 127 and 0 that correspond, respectively, to voltage amplitudes between 0 and 2.5 V.[5]

(2) A given grayscale level corresponds to a square-wave voltage waveform of a corresponding amplitude that switches symmetrically around 0 V. The switching speed is user selected using the SLM control software. We use the manufacturer-recommended 2 kHz switching rate, which is selected to be much faster than the relaxation time of the LC molecules.

(3) In the speedup algorithm, the only values of spiking voltage used are from those values that correspond to the grayscale values of the SLM addressing circuit. Therefore the voltages applied are from the same range of values that one would normally, apply even if one did not employ a speedup algorithm. Spiking waveforms, as we describe them here, do not drive the SLM outside its designed range and would not be expected to damage or shorten the lifetime of the SLM.

(4) The switching time of the NLC is highly variable depending on the final value of voltage applied.[9] According to Wu's model in Ref. 9, the switching time is infinite at the NLC threshold voltage V_{th}. For voltages between 0 and 1.41 V_{th} the switching time is greater than the free relaxation time (the switching time when the applied voltage is set to zero) and above 1.41 V_{th} the switching time is less than the free relaxation time and decreases with increasing voltage. As a result, for an analog-valued SLM programmed with arbitrary patterns, switching times can be expected to vary significantly.

(5) NLC switching transients are sublinear or qualitatively exponential (as sketched in Fig. 1). Therefore a superlinear speedup is possible by switching toward a final value in excess of the user-programmed target value for an SLM pixel. This is the source of the speedup provided by the spiking algorithm.

(6) None of the analog SLMs that we are familiar with includes spiking or other specialized speedup waveforms. Instead the voltage is simply stepped directly to the pixel target values, resulting in the slow switching times described in comments (4) and (5). For a manufacturer to build speedup waveforms into the addressing circuit would be complicated due to the voltage-dependent switching times [see comment (4)].

(7) The novelty in this paper is not the concept of spiking itself, but rather the ability to introduce spiking waveforms customized for each pair of pixel values between consecutive frames. The BNS SLM is a digitally frame-addressed SLM, and with an adjustable frame time of as short as 0.164 ms, it becomes possible to introduce one (or more) intermediate frames to implement spiking waveforms. One could choose to spike each individual pixel in the shortest time possible, but this would require the generation of a new frame for each resulting switching time t_s. The number of frames and amount of address data created could be impractically large. A reasonable compromise would be to switch all pixels as fast as the slowest responding pixel value. This would result in a single switching time that could be achieved by the insertion of a single transient frame between the current steady-state pixel values and the final steady-state values. It is the recognition of this form of a speedup algorithm and its implementation that we consider to be the principal contribution of this paper.

(8) In the SLM used in this study, the voltage range exceeds that required to produce the 2π phase range that we desire. This ensures that spiking can be applied even when the desired phase is at the limits of the phase range. Related to this point, the voltage range can vary depending on the wavelength used or the application (say an application that uses a π instead of 2π phase range.) Under these circumstances the spiking waveforms would need to be modified to achieve the fastest switching time t_s. In addition to

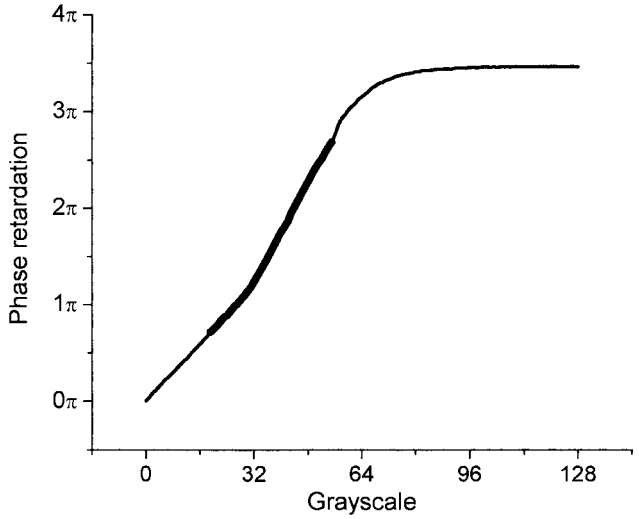

Fig. 2. Phase retardation of the SLM in steady state. The SLM is programmed to produce the values from the 2π operating range (thick curve) in steady state while the spiking voltage can be selected from the entire range (thick and thin curves) in order to speed up the switching of the SLM.

comment (6), this consideration provides a further complication for manufacturers to build speedup waveforms into their SLMs.

3. Phase Measurements

The SLM's phase response as a function of voltage and time is determined from intensity measurements with the SLM placed between two parallel polarizers that are rotated 45° from the principal axes of the LC. The light source used is a 532 nm laser. The intensity I measured on the photodetector is assumed to be modeled as

$$I(t) = I_0[1 + \cos \varphi(t)]/2, \quad (1)$$

which is the relation for a lossless birefringent crystal where phase $\varphi(t)$ is a function of time t and I_0 is the intensity of the incident beam.

In the steady state, where the grayscale level of voltage G is independent of time, the phase φ depends solely on G. The resulting function $\varphi(G)$ determined from our measurements is shown in Fig. 2. The phase can be varied continuously over $\sim 3.5\pi$. The grayscale to retardation response is essentially identical across the entire aperture of the SLM. However, the device is not flat and there is a slow spatial variation in phase (as measured in an interferometer) that varies from flat by ~ 3 waves across the aperture. The central portion of the curve in Fig. 2 corresponds to the grayscale levels from 20 to 56, which address full 2π phase range. In Section 5, when we apply the speedup method to the SLM, the steady-state phase values (which include the spatial phase correction) will only be selected from this "operating range." Also note that the phase begins to change for grayscale values less than ~ 64 (recall that voltage decreases with grayscale), which suggests that this level corresponds approximately to the threshold voltage V_{th} of the NLC.

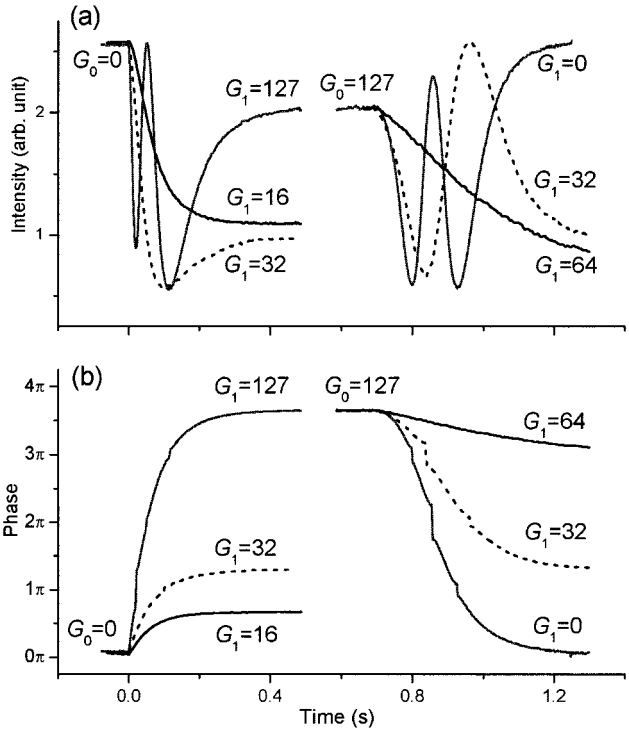

Fig. 3. Transient responses of the SLM between pairs of grayscale levels. (a) The measured intensity transients and (b) the transient phase modulation calculated from (a) using Eq. (1). Curves on the left represent the "rising case" and curves on the right represent the "falling case." Color is used in the online version of the paper to aid in separating the curves.

The transient properties of the SLM are seen by switching the address value from initial grayscale value G_0 to the final value G_1 and observing the intensity changes. Figure 3(a) shows several transient intensity responses. The curves on the left show how the intensity changes as the grayscale level $G_0 = 0$ is switched to the three final values $G_1 = 16, 32,$ and 127. We refer to switching from a lower to a higher grayscale level as the "rising case." The curves on the right side of Fig. 3(a) show transients corresponding to $G_0 = 127$ being switched to the final values of $G_1 = 0, 32,$ and 64. We refer to this case as the "falling case." The phase corresponding to these intensity curves is plotted in Fig. 3(b). The unwrapped phase has been calculated by inverting Eq. (1) under assumptions of continuous and monotonic changes in the phase as a function of time. Discontinuities in the phase occur at the peaks and valleys of the intensity. These discontinuities are a result of the photodetector not recording the extreme values of intensity due to its slow (15 ms) rise time. The degree to which this detector's rise time influences the measurement of the transient phase response is small. Details of its influence are deferred to in Appendix A. Of greatest significance to the speedup algorithm, note that the transient phase shows a sublinear response [see Section 2, comment (5)].

4. Numerical Model of the Transient Phase Modulation

In this section we describe the regression of the transient phase response curves to model functions and then in Section 5 we use these functions to solve for the transition time to change between the current value and the desired final value of phase.

The phase for the rising case [left side of Fig. 3(b)] is well modeled by the exponential function

$$\varphi(t) = \varphi_0 + (\varphi_1 - \varphi_0)\left[1 - \exp\left(-\frac{t - t_0}{\Delta t}\right)\right], \qquad (2)$$

where φ_0 is the steady-state phase (as given by the curve in Fig. 2) corresponding to grayscale level G_0 up to initial time t_0 and φ_1 is the steady-state phase corresponding to grayscale level G_1 that is applied from t_0 onward. The one unknown parameter, the time constant Δt, is estimated by performing a least-squares fit of Eq. (1) with a phase argument of the form of Eq. (2). The values of the time constant have been determined for several pairs of values of initial and final gray levels G_0 and G_1. Some of the values of the time constant are graphed in Fig. 4. Note that a small change in the grayscale level usually results in a larger value of time constant than does a small change in address level. This trend is especially pronounced around the final grayscale value of 64. For small phase changes (especially initial gray levels close to 64) transition times can be greatly accelerated by spiking. Then, not only is Δt much smaller (for instance, less than 70 ms at $G_1 = 127$ compared to 140 ms at $G_1 = 64$, from Fig. 4) but by increasing the transient phase range from $\varphi_B - \varphi_0$ to $\varphi_1 - \varphi_0$ for the duration of the spiking frame enables φ_B, the desired phase value in the speedup algorithm, to be reached much faster than without the spiking frame [see Section 2, comment (5)]. In Section 5 these time constants and their dependence on pairs of values G_0 and G_1 are used to specify the rising case portions of the spiking waveforms.

For the falling case transient phase [curves on the right side of Fig. 3(b)] there appears to be an initial quadratic trend. We found a satisfactory piecewise fit to the phase φ to be a quadratic (for $\varphi_H < \varphi < \varphi_0$), a line (for $\varphi_M < \varphi < \varphi_H$), and an exponential (for $\varphi_1 < \varphi < \varphi_M$), where the breakpoints between the three curves are expressed as $\varphi_H = 0.85\varphi_0 + 0.15\varphi_1$ and $\varphi_M = 0.5\varphi_0 + 0.5\varphi_1$. The equation for the piecewise curve is then written as

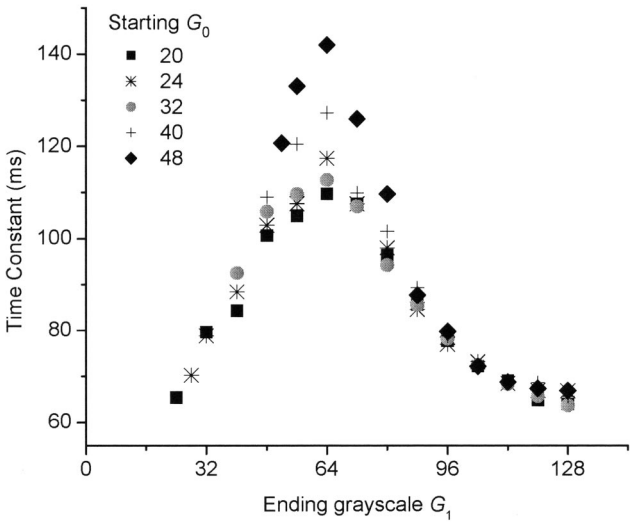

Fig. 4. Measured time constants for the rising case.

where Δt_1 and Δt_2 both correspond to scaling parameters, and also the time extent of the quadratic and linear pieces, respectively. The scaling parameter Δt_3 is interpreted in a similar way as is Δt in Eq. (2). These three parameters were found for curves similar to those in Fig. 3(b) data by least-square fitting of Eq. (1) with the phase model of Eq. (3). The values found for the parameters are presented in Appendix A. The maximum value considered is $V_0 = 56$ since this corresponds to the maximum steady-state phase value that we program on the SLM.

5. Prescription of the Spiking Waveforms

With respect to Fig. 1, for a single pixel the goal would be to switch the steady-state phase of a single pixel φ_A to φ_B in the minimum switching time t_s. This is accomplished by selecting the largest grayscale value ($G_1 = 127$ for our SLM). This grayscale value produces the transient phase response $\varphi_{s1}(t)$ (the dotted curve in Fig. 1). When the phase reaches the desired value φ_B, the grayscale is switched to the value that corresponds to steady-state phase φ_B, shown by the solid horizontal line. If this method were applied to all the pixels of the SLM, it would require using a number of different values of duration t_s for the spiking waveforms. Given that the SLM is a frame-addressed device, this would require the loading of a new frame on the SLM for every value of t_s [see Section 2, comment (7)].

$$\varphi(t) = \begin{cases} \varphi_0 + (\varphi_H - \varphi_0)\left(\dfrac{t - t_0}{\Delta t_1}\right)^2, & t_0 < t \le t_0 + \Delta t_1, \\ \varphi_H + (\varphi_M - \varphi_H)\left(\dfrac{t - t_0 - \Delta t_1}{\Delta t_2}\right), & t_0 + \Delta t_1 < t \le t_0 + \Delta t_1 + \Delta t_2, \\ \varphi_M + (\varphi_1 - \varphi_M)\left[1 - \exp\left(-\dfrac{t - t_0 - \Delta t_1 - \Delta t_2}{\Delta t_3}\right)\right], & t > t_0 + \Delta t_1 + \Delta t_2, \end{cases} \qquad (3)$$

Table 1. Measured Switching Times with and without Spiking

Case	With Spiking[a] t_s (ms)	Without Spiking t_s (ms)
0-2π rise	67	320
2π-0 fall	98	420
0-π rise	28	250
π-0 fall	46	500

[a]Spiking grayscale is 127 for rising case and 0 for falling case.

Rather than filling the SLM memory with a large number of frames, the speedup method can be considerably simplified by selecting spiking voltages for the SLM pixels so that all pixels switch from their beginning to their final steady-state phase at the same value of time t_s. The value of t_s would then be selected to be the minimum possible switching time (from all available grayscale levels) for the slowest switching pixel. For example, in Fig. 1, by selecting a smaller value of $G_1 (G_1 < 127$ for our SLM) than the maximum value, then the transient phase $\varphi_{s1}(t)$ can be slowed down to $\varphi_{s2}(t)$, resulting in a switching time t_s that also can be achieved at other pixels by slower responding combinations of phase φ_A and φ_B in successive frames.

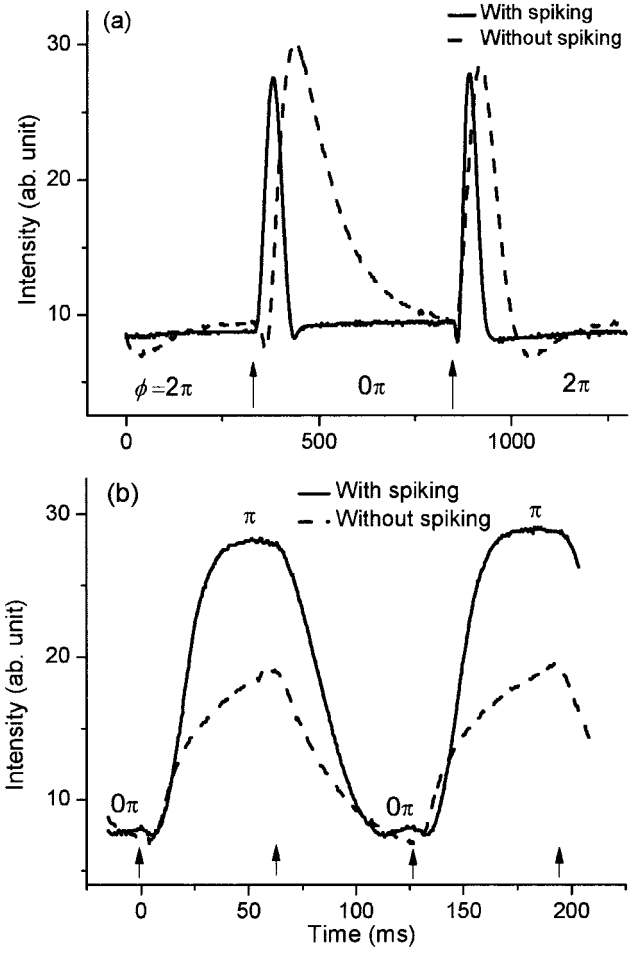

Fig. 5. Transient intensity of the SLM for switching between grayscale levels of (a) 20 and 56 for a 2π transition and (b) 20 and 39 for a π transition. In both (a) and (b) the solid curves show the transient intensity with the spiking frame and the dashed curves show the corresponding curves without spiking.

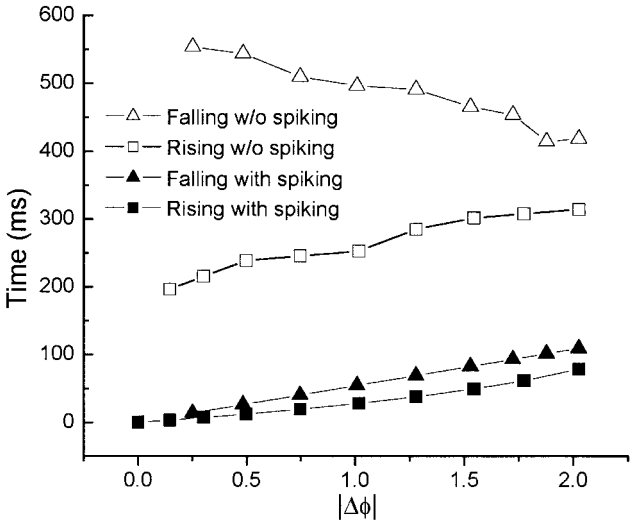

Fig. 6. Minimum switching time to achieve a given phase shift. The rising phase starts from grayscale 20, and the spiking grayscale used is 127. The falling phase starts from grayscale 56, and the spiking grayscale used is 0.

We calculate the solution for the spiking voltage for the rising case by finding the minimum absolute difference between the pixel phase $\varphi(t_s)$ and the desired phase φ_B at the switching time t_s as a function of the fixed model parameters φ_0 and the dependent pair of variable parameters φ_1 and Δt . For the falling case the four variable model parameters φ_1, Δt_1, Δt_2, and Δt_3 are linked. Thus the search is over values of $\varphi(t_s)$ of the form of Eq. (2) for the rising case and of the form of Eq. (3) for the falling case. The number of model functions examined depends on the value of φ_0 or its corresponding grayscale level. For our operating range of grayscales (from 20 to 56), depending on the current pixel grayscale level, there are 71–107 model functions for the rising case and 21–56 model functions for the falling case that can be examined to determine the closest match of $\varphi(t_s)$ to φ_B . Needless to say, not all model functions, and based on the search method, only a few functions need to be evaluated. However, the search methods themselves were not a focus of this investigation. Even using the most basic sequential search of the values of $\varphi(t_s)$ our algorithm running on a Pentium 4 computer (2.4 GHz, 1 GB-DRAM) can design the spiking voltages for the entire 262 144 pixel SLM in under 1 s.

6. Demonstrations of the Use of Spiking Waveforms

The most direct demonstration of the speedup is to compare, for a single pixel, the switching transients that result with and without the use of spiking. The SLM is configured as an intensity modulator as in Section 3. The speedups in switching time are summarized for four cases (Table 1). These values were measured from the oscilloscope traces in Fig. 5 of the

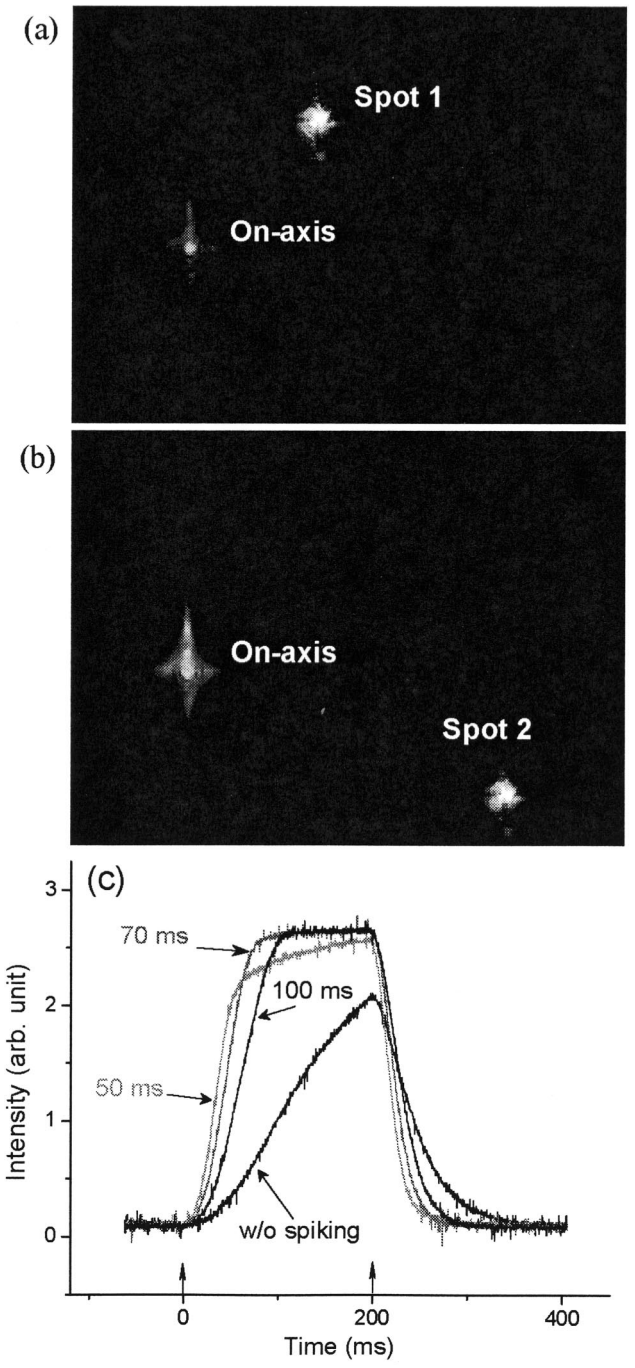

Fig. 7. Diffractive beam switching experiment. (a), (b) Diffraction patterns of spot 1 and spot 2 shown in the steady state following completion of the switching transient (Ref. 11). (c) Transient intensity of diffracted spot 2 for different durations of the intermediate spiking frame. Color is used in the online version of the paper to aid in separating the curves.

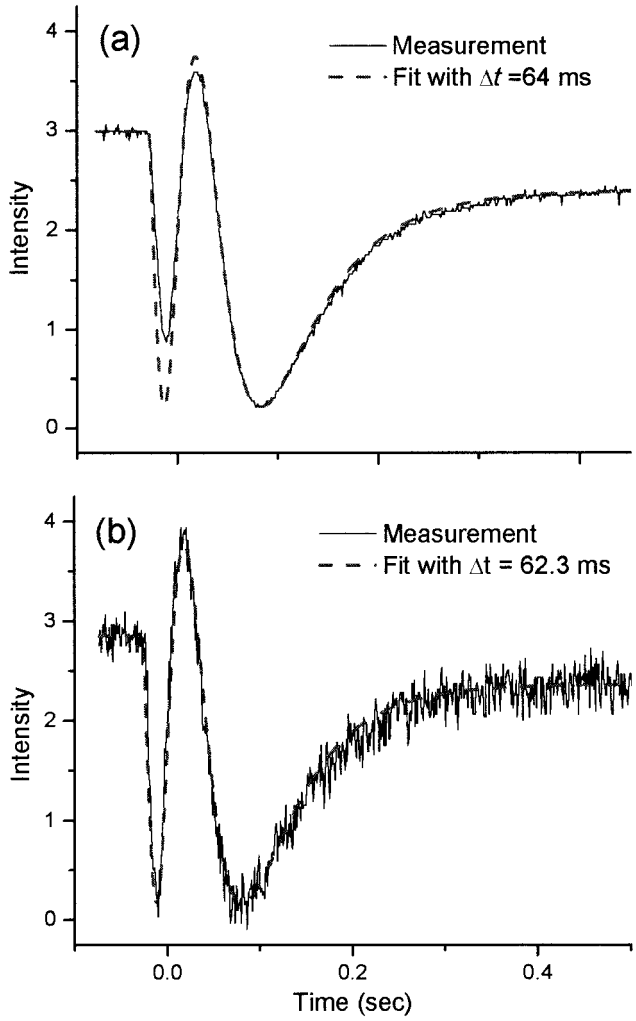

Fig. 8. Comparison of (a) a slow detector and (b) a fast but noisy detector in following the transient intensity of the SLM as it is switched from grayscale level 0 to 127. Both measured responses and the resulting least-squares fit to Eq. (1) are shown.

detected intensity (per the experimental setup in Section 3) for repetitive switching between phases 0 and 2π (grayscale levels 20–56), and 0 and π (grayscale levels 20–39). Also, Fig. 6 summarizes the rise and fall times that were measured for all values of phase transition between 0 and 2π . Spiking leads to significant speedups in all cases. Note that for these experiments, and for the experiments that follow, that the switching time is defined as the time required to reduce the initial phase difference $\varphi_B - \varphi_A$ by 95% or to $(\varphi_B - \varphi_A)/20$.

In a second demonstration the SLM is configured as a phase modulator[8] and used to diffractively steer the incident laser beam. For this configuration the polarizers are removed from the intensity modulator configuration, and the laser polarization is aligned with the extraordinary axis of the LC in the SLM. The light reflected from the SLM is Fourier transformed with a 120 mm achromat. In addition to recording the image of the focal plane on a CCD camera, a photodetector is positioned to record the intensity from a single focused spot. Two linear phase ramps are designed and implemented on the SLM. This design includes two steady-state frames and two intermediate spiking frames, as well as compensation for spatial phase errors in the SLM by using a spatial phase calibration procedure.[8] The patterns are designed to produce spot 1 at (1/8, 1/8) and spot

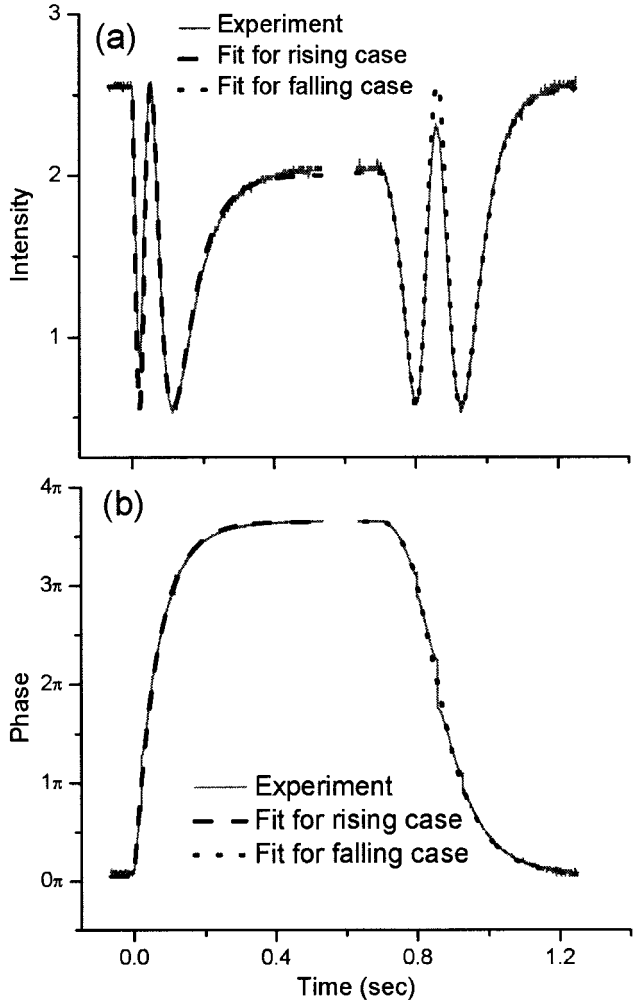

Fig. 9. Quality of the least-squares fits. (a) Intensity transients for switching between grayscale 0 and 127 (curve on left) and 127 to 0 (curve on right) together with the least-square fits. (b) The corresponding transient phase from inverting Eq. (1) for both the measurements and the fits in (a).

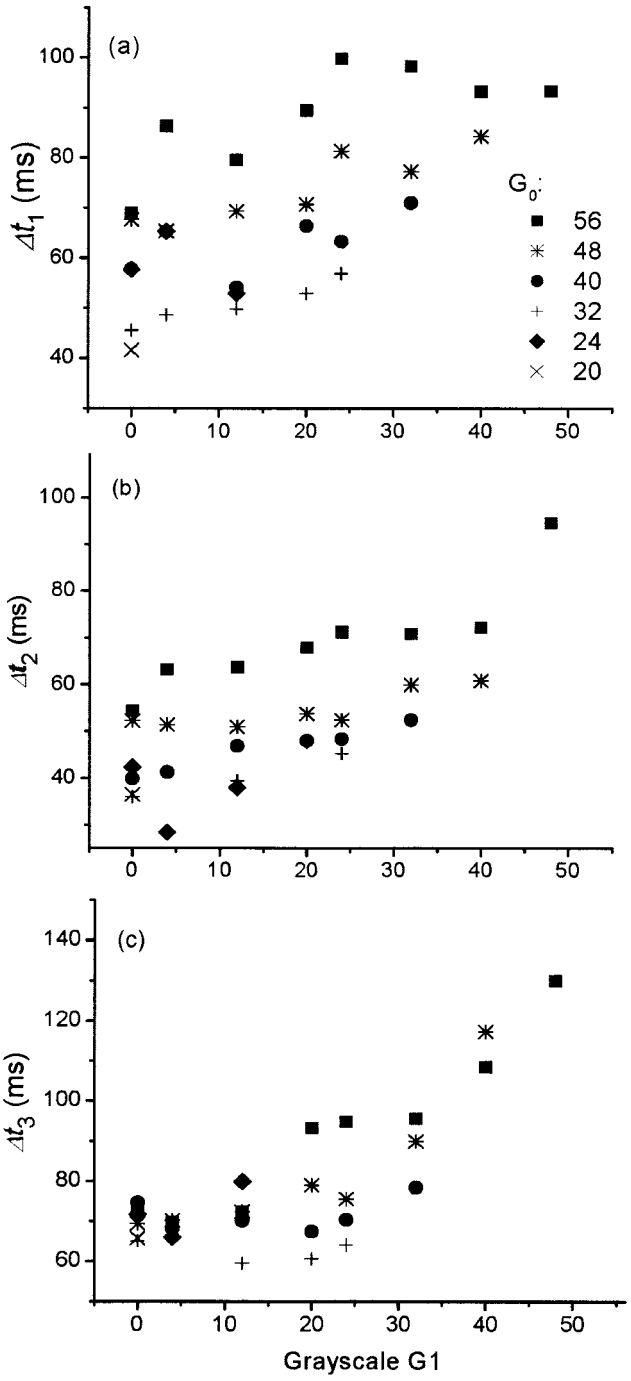

Fig. 10. Measured fitting parameters for Eq. (3) that describe the transients for the falling case.

2 at $(2/7, -1/8)$ in the x, y plane, where unity corresponds to the Nyquist frequency (i.e., 1/2 is the grating frequency of the pixels.) The patterns are switched repetitively between the two spot locations. The detector is positioned to measure the transient intensity of spot 2. Figure 7 shows the diffraction patterns recorded with the CCD camera and the transients for various values of spiking frame duration t_s. For a 100 ms spiking frame the rise time is 104 ms and the fall time is 102 ms, which is considerably faster than without spiking. Shortening the switching duration used in the spiking frame reduces the rise time to 77 ms and the fall time to 71 ms. Apparently spot 2 can be nearly completely switched to its steady-state intensity as a result of only a small fraction of phase transitions being close to 2π. However, designing the spiking frame for 50 ms leads to an initially faster transient followed by the very slow rise time after the steady-state frame is applied. In 200 ms the spot intensity only reaches 92% of the steady-state intensity. (If it is desirable to have this initially faster transient, it would be possible to design for speedup with two, or even more, spiking frames in sequence.) The fall time for the 50 ms spiking frame is quite fast, in part due to the slowest pixels not reaching their final values during the rising transient. The fact that the rise and fall times are different is somewhat of a surprise given that the number of upward transitions and downward transitions in switching between two rather arbitrary phase patterns would be expected to be equal.

An additional note of interest is that the on-axis spot is more intense when the spot is diffracted to location 2 than when it is diffracted to location 1. The increased on-axis light is a result of the expected decrease in diffraction efficiency with increase in spatial frequency.[10] In addition to speeding up the transition, movies of the diffraction patterns[11] show that spiking reduces both the time that the "ghost" or residual spot remains and the amount of energy that is scattered into the zero-order, on-axis spot.

Also, while not the focus of the study, environmental stability of the speedup calibration and the NLC is briefly noted. The two-spot beam switching experiment was repeated over 20 times over a 3-month period using the same calibrations (both speedup and spatial phase correction). There were no noticeable changes between the measured intensities or the switching times. Over this same time the laboratory temperature is known to have varied between 18° and 23 °C. Based on these preliminary observations we conclude that the SLM and the calibrations are fairly insensitive to modest temperature changes and aging effects.

7. Conclusions

The introduction of a single spiking frame between each desired steady-state grayscale addressing frame provides a fairly simple way to increase the switching speed of LC SLMs that have a phase range significantly in excess of one wave of retardation. For the specific experimental device studied, the switching time was reduced from a minimum of 400 ms down to a maximum of 77 ms for the rather arbitrary phase patterns designed to switch between two spots. To our knowledge, this is the first time a speedup algorithm has been reported that takes into account the need to simplify the address signal and memory requirements of a frame addressed SLM. The accelerated switching speed, which results from the introduction of a single intermediate spiking frame, can be used to increase speed and diffraction efficiency of analog NLC phase modulators. Such improvements in SLM performance could be usefully employed to enhance real-time systems such as multitarget laser designators and multibeam optical tweezers systems.[6,12]

Appendix A

The detector used has a measured rise time of 15 ms. It does not closely follow the most rapid variations in intensity, e.g., when the SLM is switched from grayscale 0 to grayscale 127, as shown in Fig. 8(a). This result can be compared with the result for a faster switching, but noisier detector in Fig. 8(b). The fit for the relaxation time model parameter Δt (see Section 3) gives a value of 64 ms when using the measurement from slow detector and a value of 62.3 ms when using the measurement from the fast detector. The closeness of the values is due to the fact that the slow detector does closely track the signal for all but the fastest portions of the signal. For smaller grayscale value changes the signals from the two detectors track even more closely.

Even without including the detector rise time in the fitting algorithm, the rising case and falling case fitting parameters prove to be sufficiently accurate to obtain close fits to the phase transients in all cases. The worst-case results (for grayscale transitions from 0 to 127 and back to 0) are shown in Fig. 9. The phase in Fig. 9(b) is well fit across the entire extent of the curve while the intensity in Fig. 9(a) is not well fit at the most rapid intensity changes. Since the phase measurement in Fig. 9(b) is calculated by inverting Eq. (1) the time lag (of up to 15 ms on a vertical slope) due to the detector rise time is not included in this comparison. If the additional step of deconvolving the detector response had been performed, its effect would be difficult to see on the phase plot in Fig. 9(b).

Figure 10 presents the set of three fitting parameters Δt_1, Δt_2, Δt_3 for the falling case that were measured for transitions between various pairs of grayscale values. Recall that an entire set of parameters defines the single function in Eq. (3).

This study was supported by the U.S. Missile Defense Agency on contract F19628-02-C-0083 through the U. S. Air Force. D. J. Cho received partial support from Ajou University.

References

1. Boulder Nonlinear Systems, Inc.; http://www.bnonlinear.com/products/XYphase/data/XYPhase.pdf
2. P. J. Bos and K. R. Beran, "The pi-cell, a fast liquid-crystal optical switching device," Mol. Cryst. Liq. Cryst. **113,** 329–339 (1984).
3. A. K. Kirby and G. D. Love, "Fast, large and controllable phase modulation using dual frequency liquid crystals," Opt. Express **12,** 1470–1475 (2004).
4. S. T. Wu and C. S. Wu, "High-speed liquid-crystal modulators using transient nematic effect," J. Appl. Phys. **65,** 527–532 (1989).
5. J. E. Stockley, Boulder Nonlinear Systems, 450 Courtney Way, No. 107, Lafayette, Colo. 80026 (personal communication, 2005).
6. H. Melville, G. F. Milne, G. C. Spalding, W. Sibbett, K. Dholakia, and D. McGloin, "Optical trapping of three-dimensional structures using dynamic holograms," Opt. Express **11,** 3562–3567 (2003).
7. D. J. Cho, S. T. Thurman, J. T. Donner, and G. M. Morris, "Characteristics of a 128 × 128 liquid-crystal spatial light modulator for wave-front generation," Opt. Lett. **23,** 969–971 (1998).
8. X. Xun and R. W. Cohn, "Phase calibration of spatially nonuniform spatial light modulators," Appl. Opt. **43,** 6400–6406 (2004).
9. S. T. Wu, "Liquid Crystals" in *Handbook of Optics Vol. 2,* M. Bass, E. W. Van Stryland, D. R. Williams, and W. L. Wolfe, eds. (McGraw-Hill, 1995), Chap. 14, pp. 14.12–14.17.
10. R. W. Cohn, "Fundamental properties of spatial light modulators for the approximate optical computation of Fourier transformations: a review," Opt. Eng. **40,** 2452–2463 (2001).
11. A video (avi format) at http://pyramid.spd.louisville.edu/~eri/papers_pres/speedup.avi shows the transient diffraction patterns with a 70 ms spiking frame without spiking (movie on left) and with spiking (movie on right). Figures 7(a) and 7(b) shows steady state images with the same field of view as the two movies in the avi file.
12. X. Xun, X. Chang, and R. W. Cohn, "System for demonstrating arbitrary multi-spot beam steering from spatial light modulators," Opt. Express **12,** 260–268 (2004).